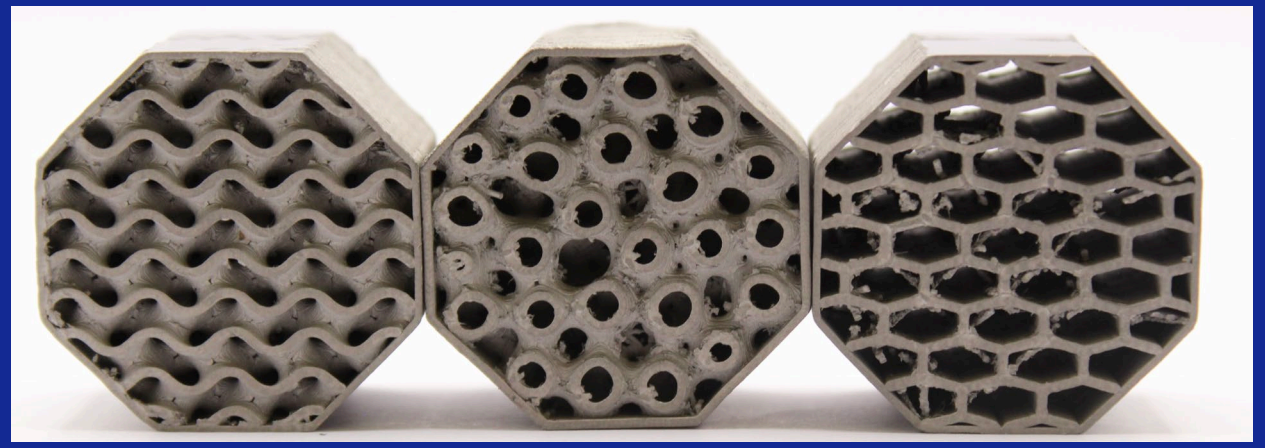
FATIH GÖZÜKÜÇÜK
JENS TELGKAMP
HAMBURG UNIVERSITY OF APPLIED SCIENCES

Additive Manufacturing and Compression Behaviour of Spherene, Gyroid and Hexagonal Cellular Structures via Metal Fused Granulate Fabrication

04.06.2026, Dresden



Gefördert durch:
Bundesministerium für Wirtschaft und Energie
aufgrund eines Beschlusses des Deutschen Bundestages

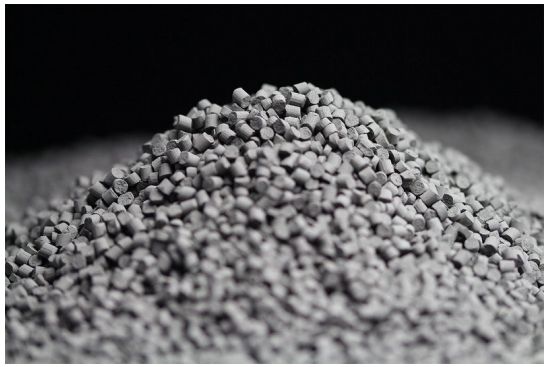
EMATec
International Conference on Emerging Applications of PM & AM Materials and Technologies

SIGNAL

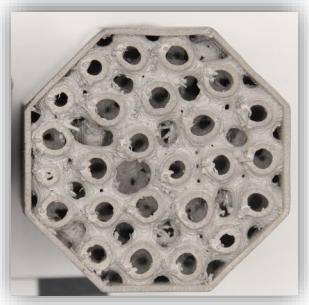
HAW HAMBURG

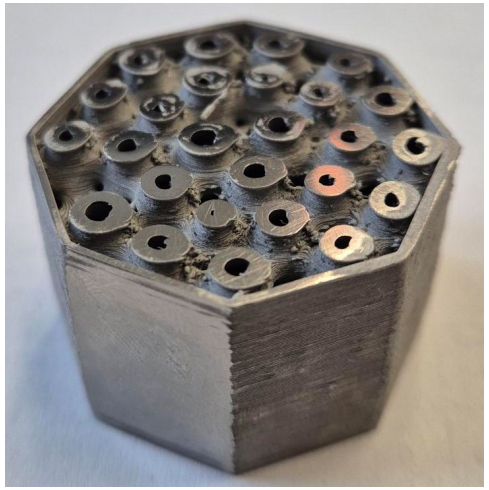
CONTENTS

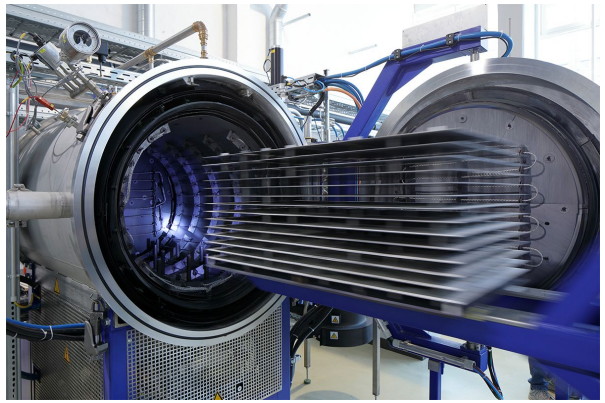
1) Material and Hardware
2) Spherene Metamaterial
3) Conventional and Developed Slicing Strategy
4) Compression Tests
5) Energy Absorption
6) Summary and Outlook













MATERIAL AND HARDWARE

Feedstock: Mixture of metal powder and polymer binder in granular form
Material: Ti-6Al-4V Feedstock from Element22 GmbH

- Use of much cheaper MIM standard materials ✅
- Higher metal powder in wt.% than filament ✅
- Enables to manufacture closed and open cellular structures ✅

Hardware: ExAM 255 granulate printer from AIM3D

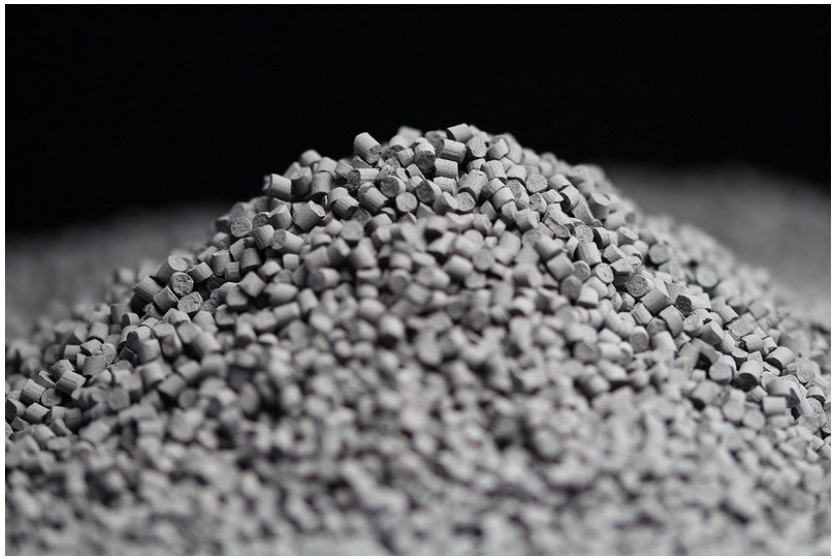


Fig.1: Granulate Ti-6Al-4V [Element22 GmbH]



Fig. 2.: Granulate Printer AIM3D ExAM 255

METHODS

WHY SPHERENE?

Advantages of Spherene, Adaptive Density Minimal Surface (ADMS)

For near-isotropic shrinkage and mechanical performance is homogeneous density distribution desired.

- TPMS geometries repeat uniformly
- Spherene's ADMS respond intelligently to stress, heat and load
- Delivers nearly isotropy for optimal stress distribution.
- Surface-conformal minimal surface technology

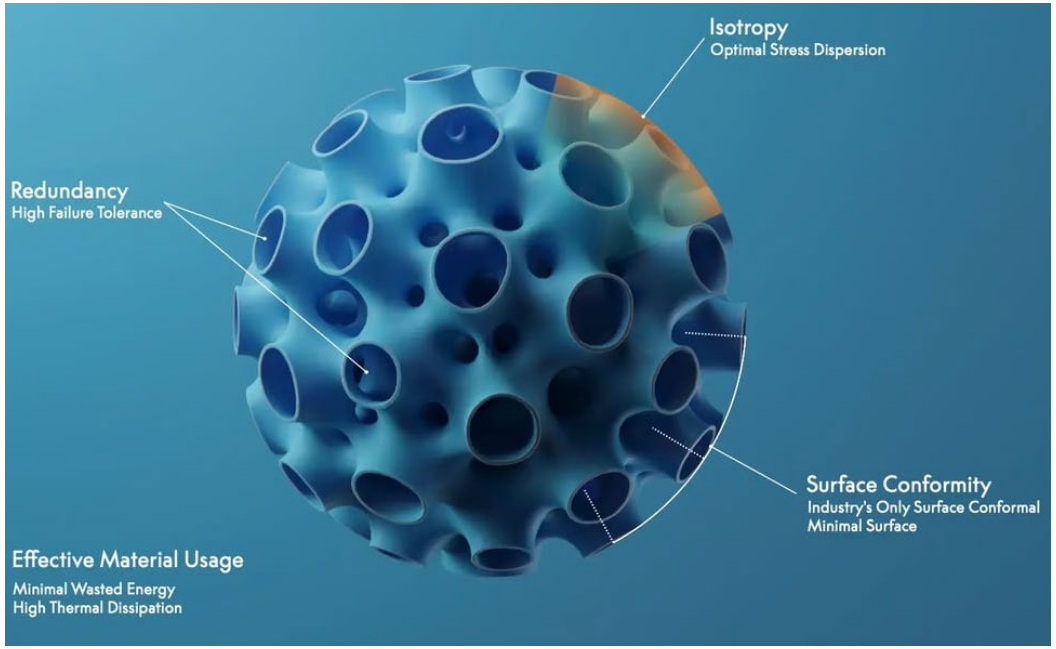


Fig. 3: Spherene metamaterial advantages

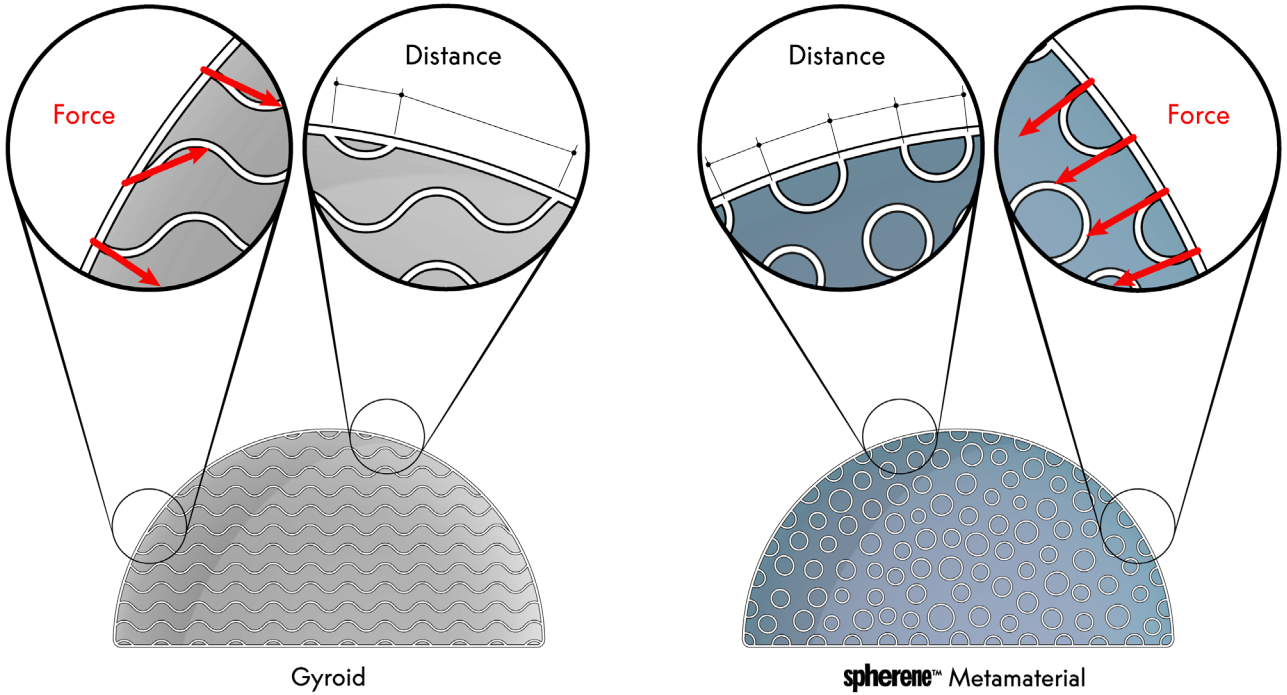


Fig. 4: Gyroid Structure and Spherene Metamaterial

GENERATED SANDWICH STRUCTURES

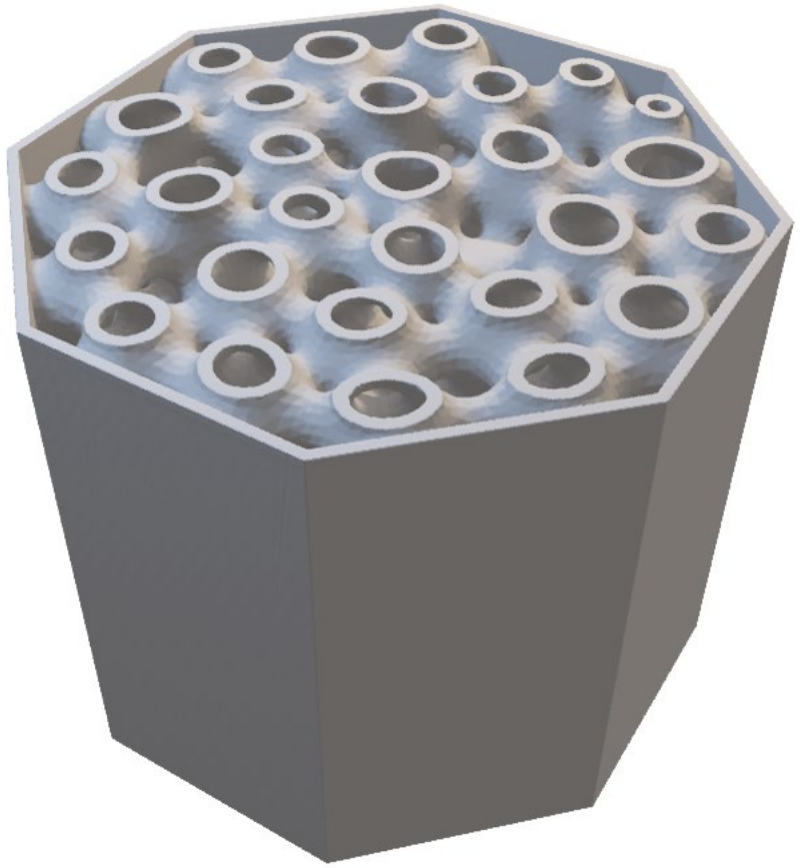


Fig. 5: 3D Design of Spherene sandwich structure in nTop

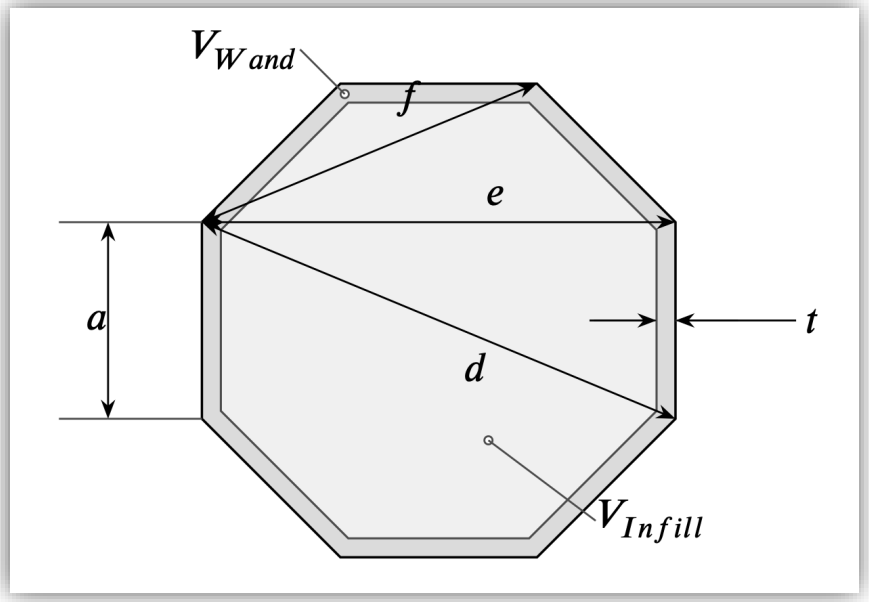


Fig. 6: Octagon Geometry

nTop Software:

Green part

Octagon geometry
- Length „e“ = 38.8 mm
- Height = 26 mm

Lattice:
- Number of cells 5 x 5 x 5
- Cell length 8 mm
- Relative density 30%

Cells:
- Spherene
- Gyroid
- Hexagonal

SLICER PROBLEM FOR METAL EXTRUSION

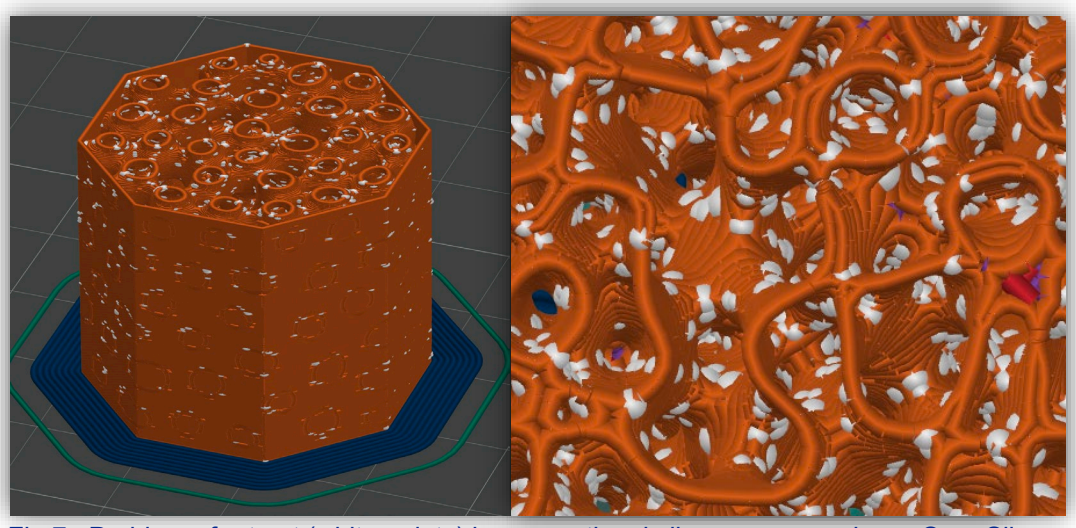


Fig 7.: Problem of retract (white points) in conventional slicer programs; here: Orca Slicer

Errors in the course of the path

Unsuitable track layouts

Abrupt track changes

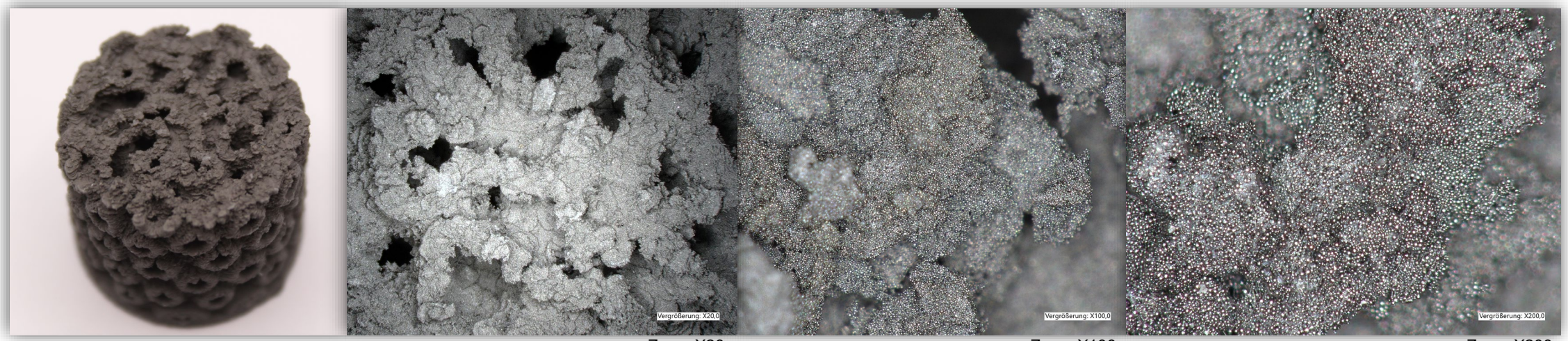
Long travel distances

Constant interruption in the strand and extrusion webs

Material behavior (Ti-6Al-4V feedstock)

Sensitive to pressure interruptions and changing extrusion rates

New slicing strategy: Slicing in python by using an AI tool



Zoom X20 Zoom X100 Zoom X200

Fig. 8: Microscopic representation of the fundamental problem with the previous printing strategy (green part)

SLICER: COMPARISON OF A LAYER INSPECTION

Orca Slicer at 12x acceleration

New slicing strategy at normal speed

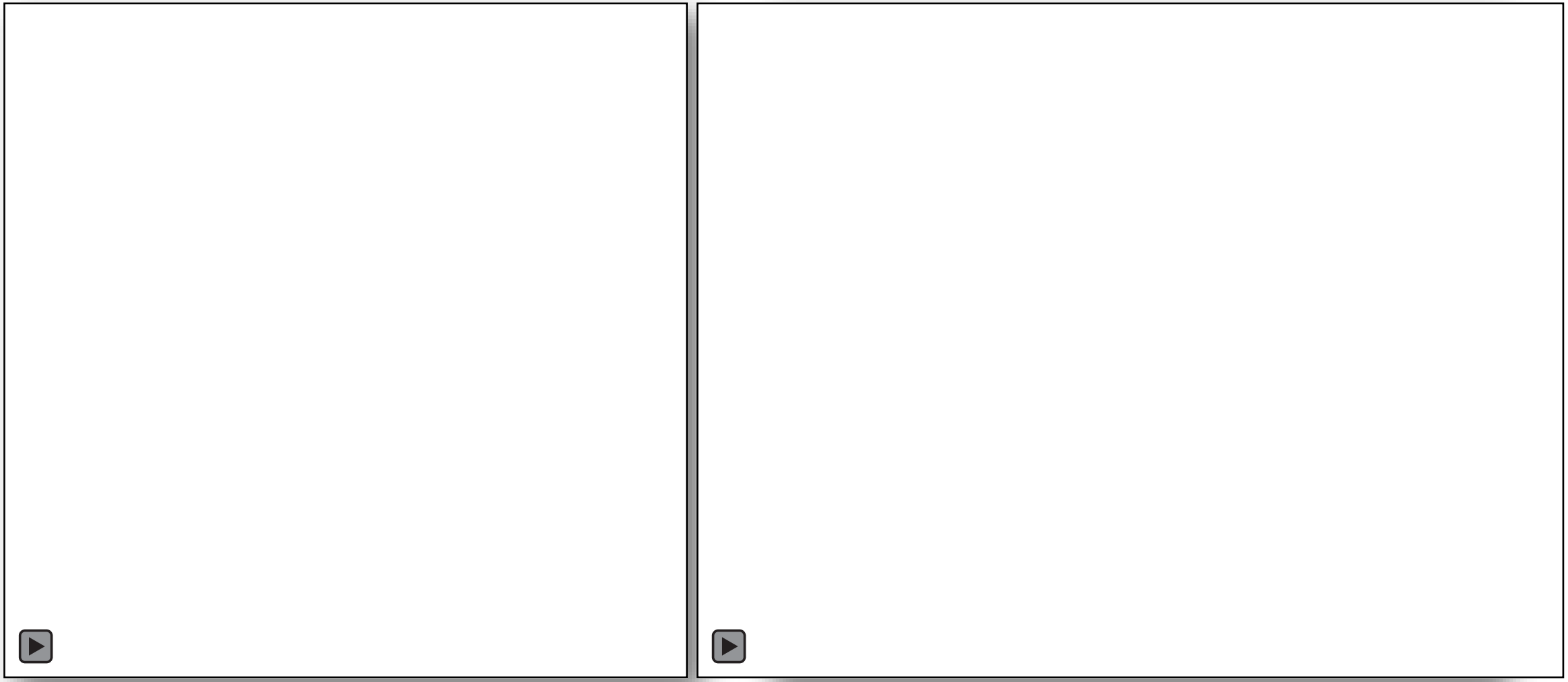


Fig. 9: Slicing on a layer: Orca slicer versus new slicing strategy

SLICER: COMPARISON OF A LAYER INSPECTION

Traditional slicer



Fig. 10: Path strategy at the Orca Slicer

Developed slicer strategy



Fig. 11: Path strategy at developed slicer

COMPARISON OF MICROSCOPE IMAGES

Before **After**

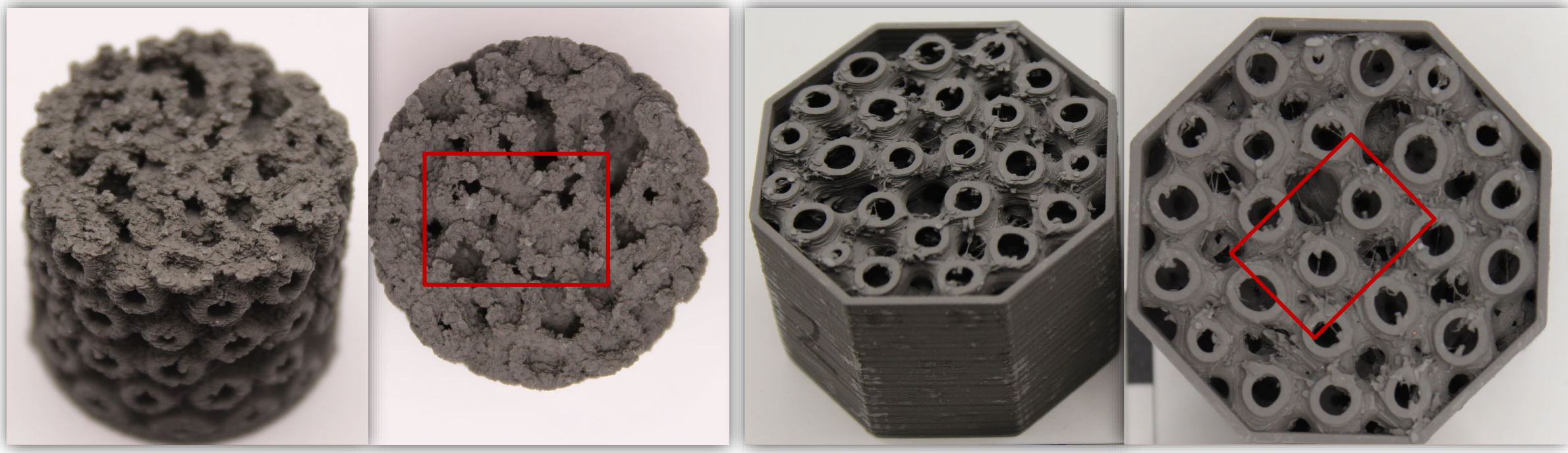


Fig. 12: Comparison of print quality (green part) - between old and new printing strategy

COMPARISON OF MICROSCOPE IMAGES

Before **After**

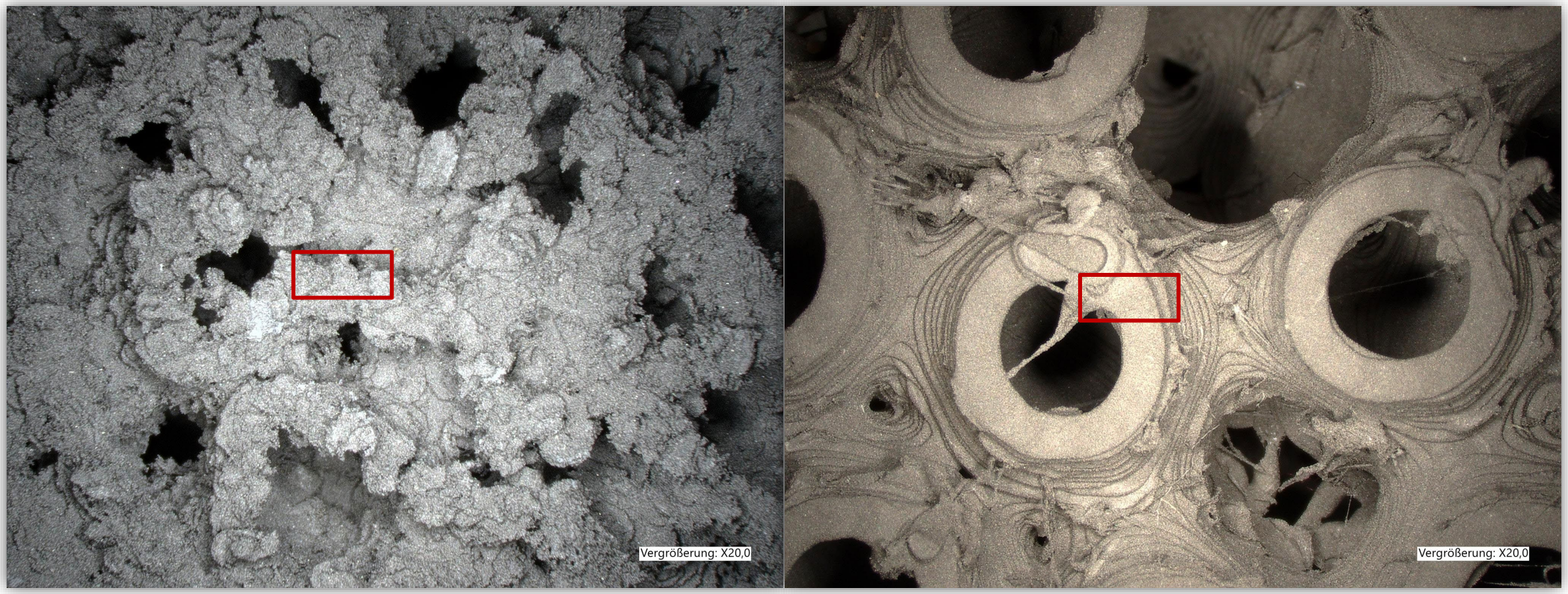


Fig. 13: Comparison of print quality - between old and new printing strategy at 20x magnification

COMPARISON OF MICROSCOPE IMAGES

Before **After**

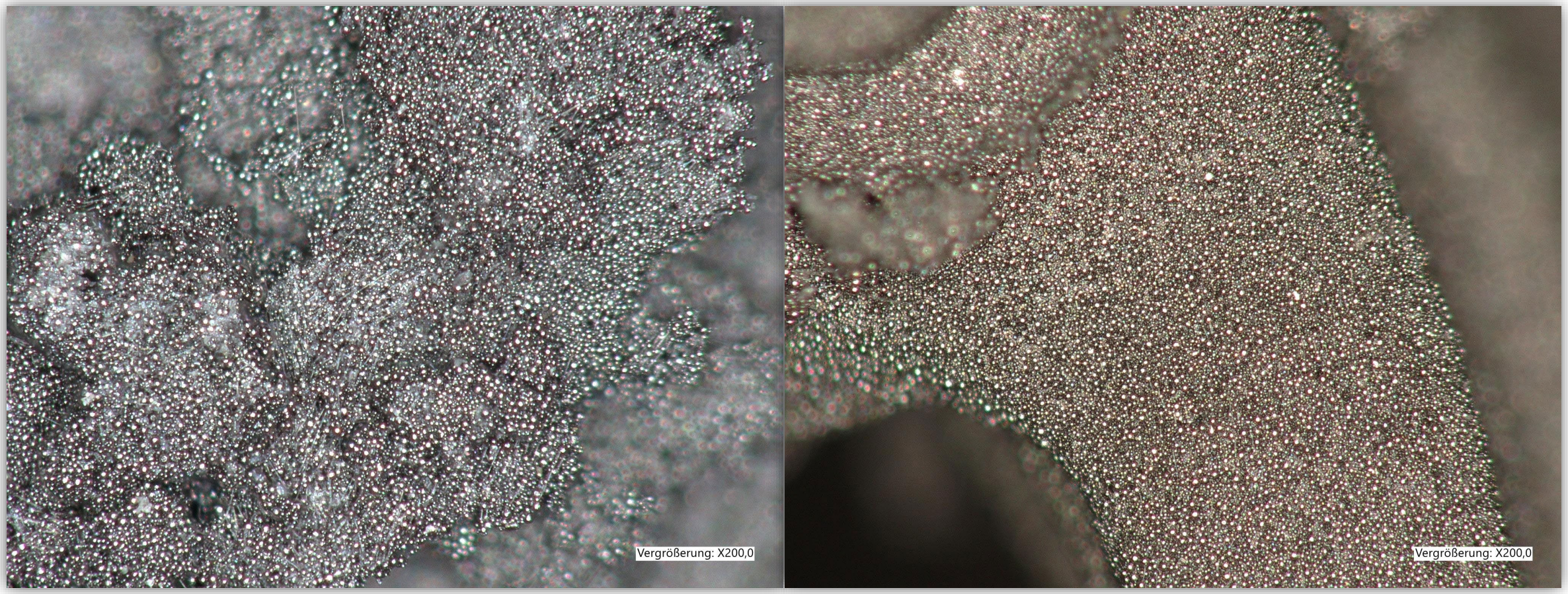


Fig. 14: Comparison of print quality (green part) - between old and new printing strategy at 200x magnification

GENERATED G-CODE IN THE PREVIEW

Spherene | Gyroid | Hexagonal

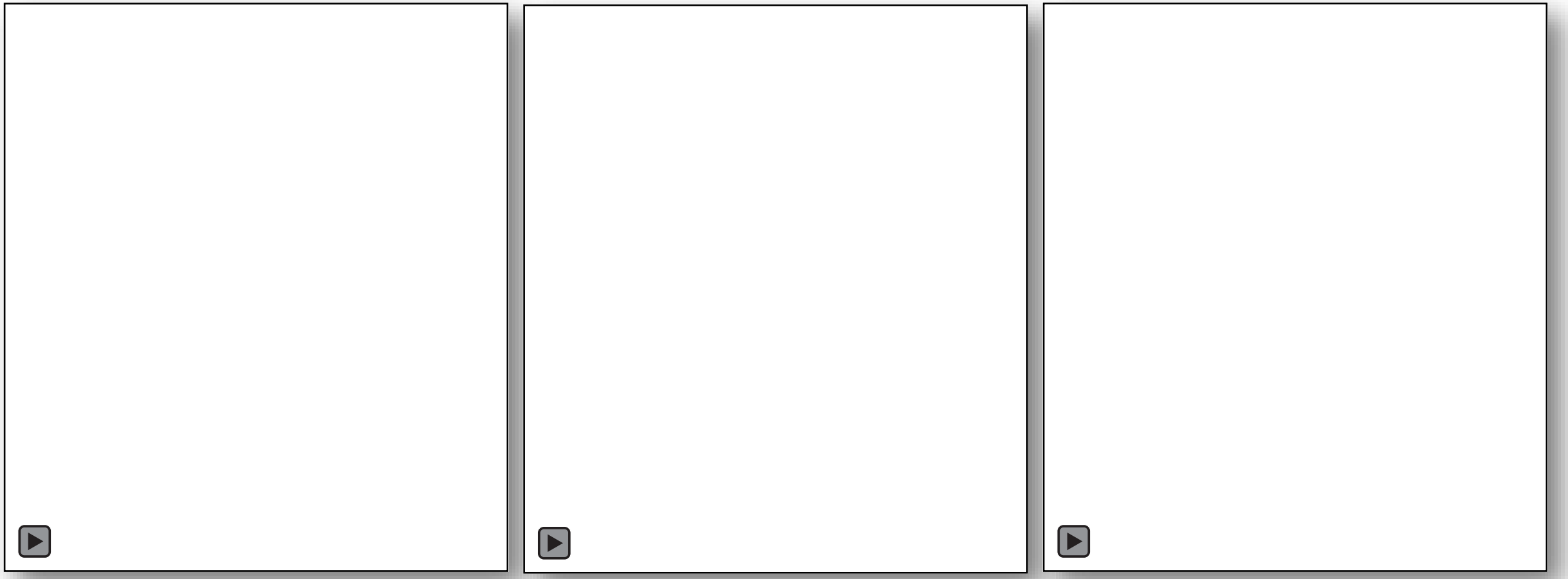


Fig. 15: Generated G-codes and associated layer inspection of the three infill structures from the slicer program

AS-SINTERED STATE

Sintering at Element 22 GmbH – Special thanks!

Density results

- Comparable density results in green and as-sintered state
- Reaching nearly 99% final density (Related to 4.43 g/cm³), in the range of MIM, Piston-based AM and above the MIM standard ASTM F2885-11

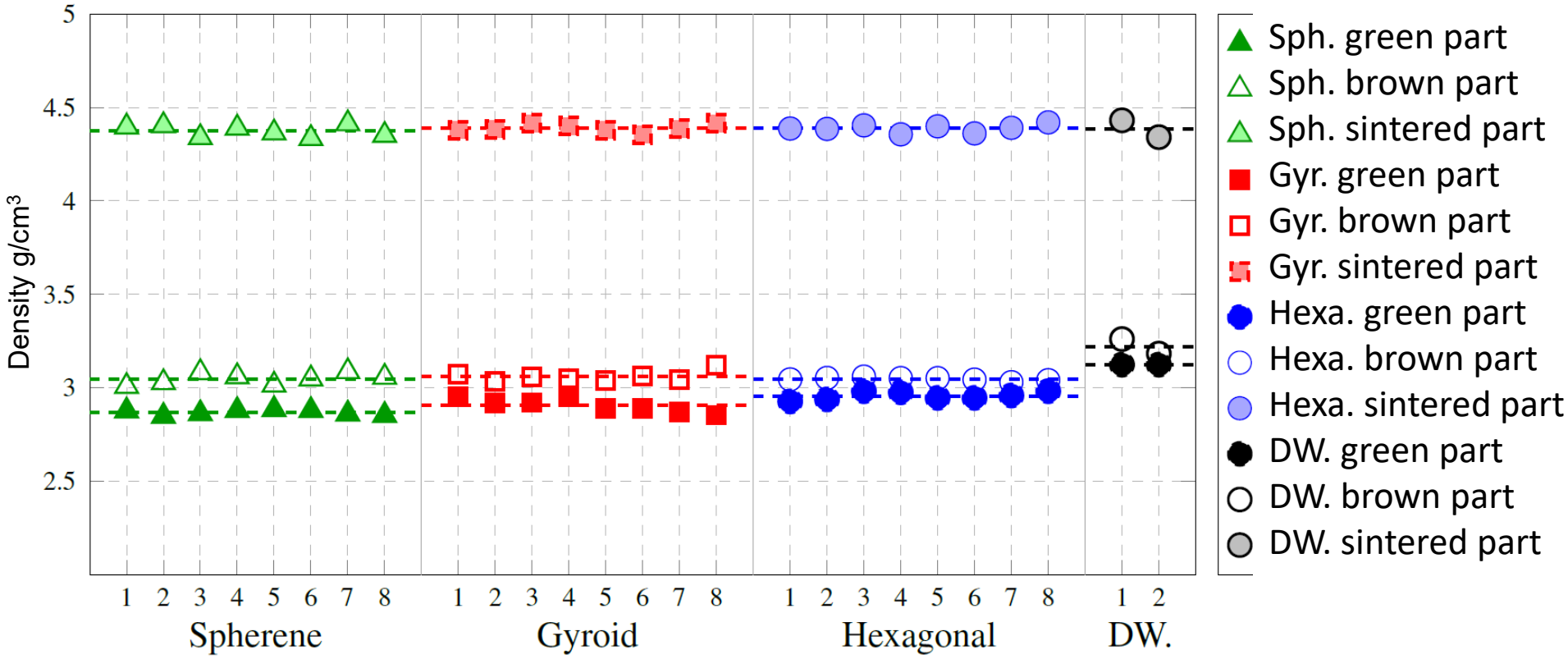


Fig. 16.: Density curve per cellular structure and sample in the states (green, brown and as-sintered) as well as density cubes, including mean value lines per state

AS-SINTERED STATE

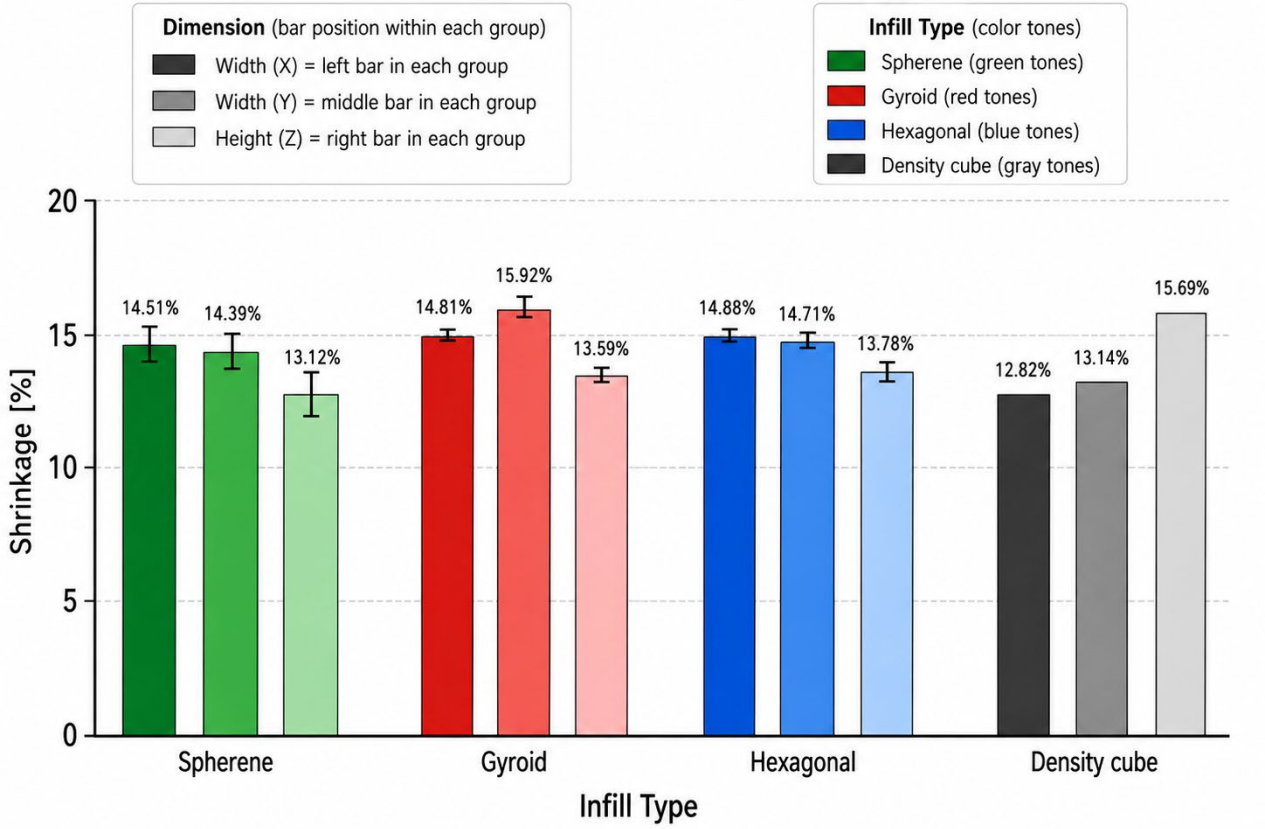


Fig 17.: Shrinkage results by infill type

Cellular structures

- Nealy isotropic shrinkage in x and y for Spherene and hexagonal
- Low shrinkage in z

Density Cuboid sample

- Low shrinkage rates in x and y
- High shrinkage in z for



Fig. 18: Representation of the change in volume, based on a green to a sintered part

COMPRESSION TEST: SAMPLE OVERVIEW

Max. load 100 kN,
3 replication
Displacement-controlled
Loading and unloading at
0,5 % | 1 % | 2 % | 3 %
| 4 % | 5 % | 10 %| 30 %

Samples
1-3 at 0°
4-6 at 45°

Spherene conforms perfectly to the outer shell and internal core

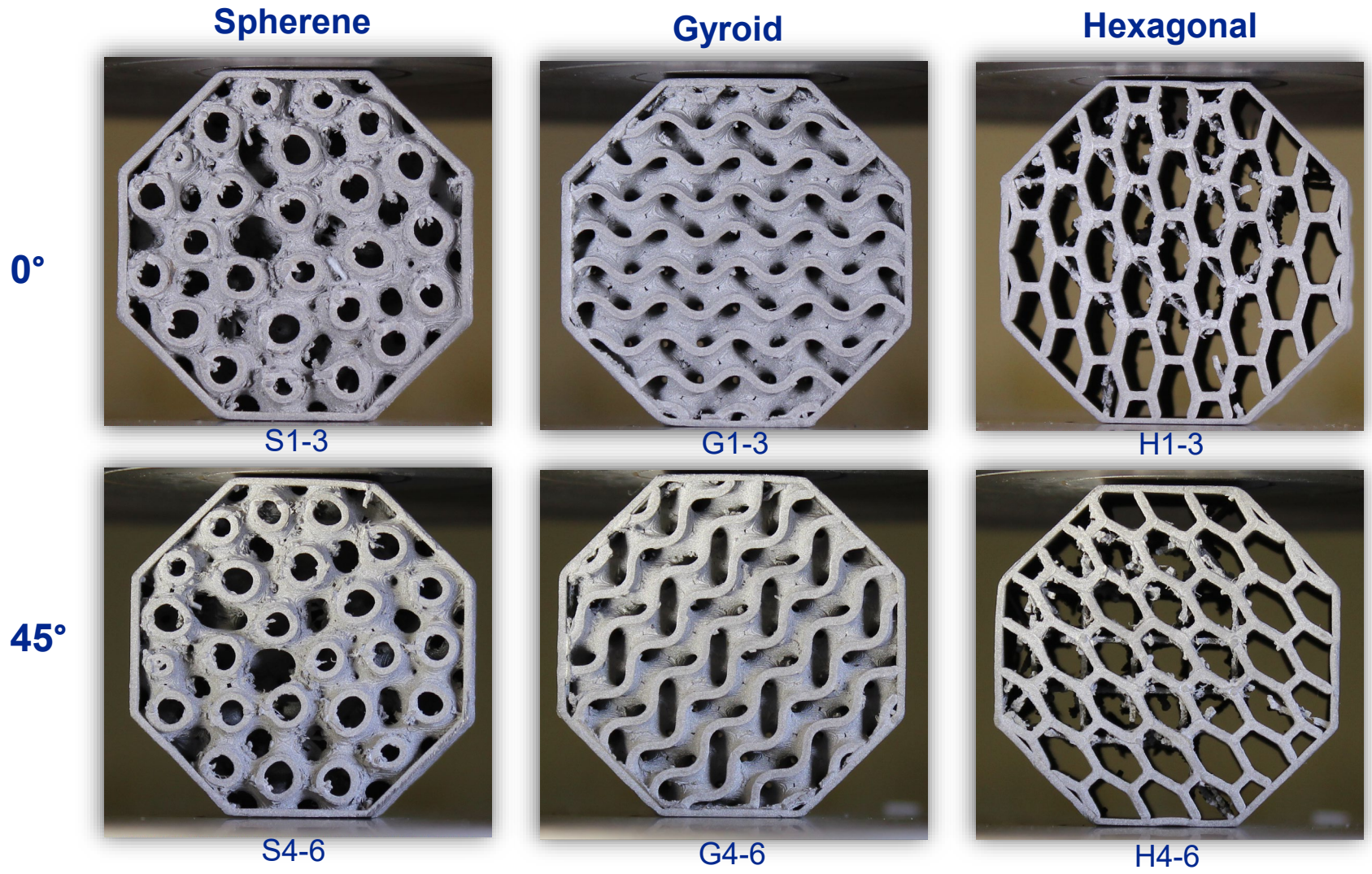


Fig. 19: Representation of the infill types in the loading direction of the pressure test

SPHERENE

Spherene: progressive collapse and controlled energy absorption

- Fmax ≈ 64 kN at 5.47–5.98% compression
- More stable post-peak response, especially for 45° orientation
- Gradual force recovery due to interaction of collapsed cell walls

Hypothesized regions in the compression response of cellular structures (I initial settling), (II – elastic dominated), (III – cell walls begin to collapse), (IV - collapse of cell walls), (V - cell walls interact)

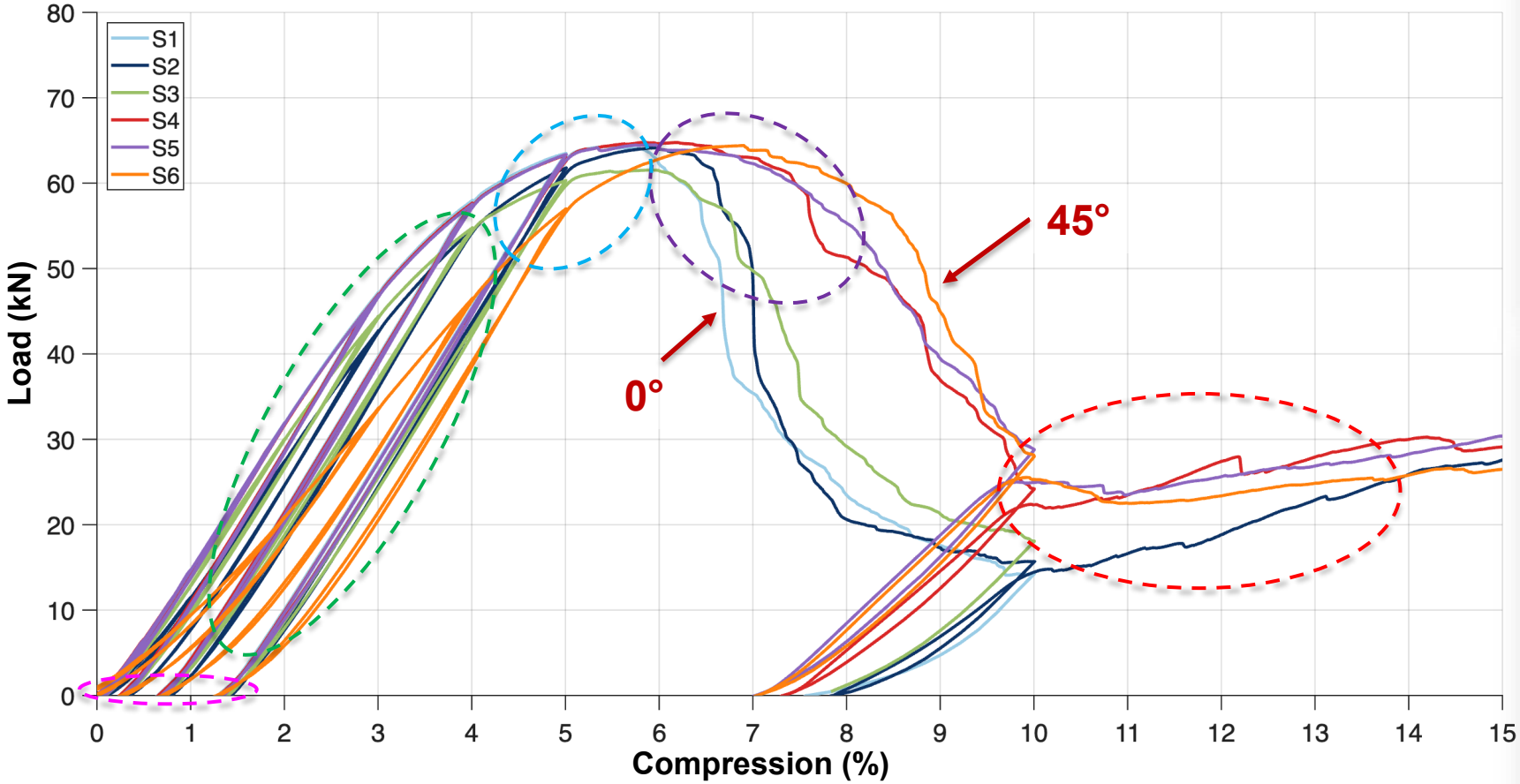


Fig. 20: Force–compression diagram of Spherene cellular structures, showing loading/unloading response of samples S1–S6

GYROID

Gyroid: higher peak load and broader load-bearing plateau, especially at 45°

- Fmax ≈ 72–76 kN
- Peak reached at about 5–7% compression
- 45° orientation shows the most stable plateau behaviour
- Collapse followed by cell-wall interaction at higher compression

Hypothesized regions in the compression response of cellular structures
(I initial settling), (II – elastic dominated), (III – cell walls begin to collapse
(IV - collapse of cell walls), (V - cell walls interact)

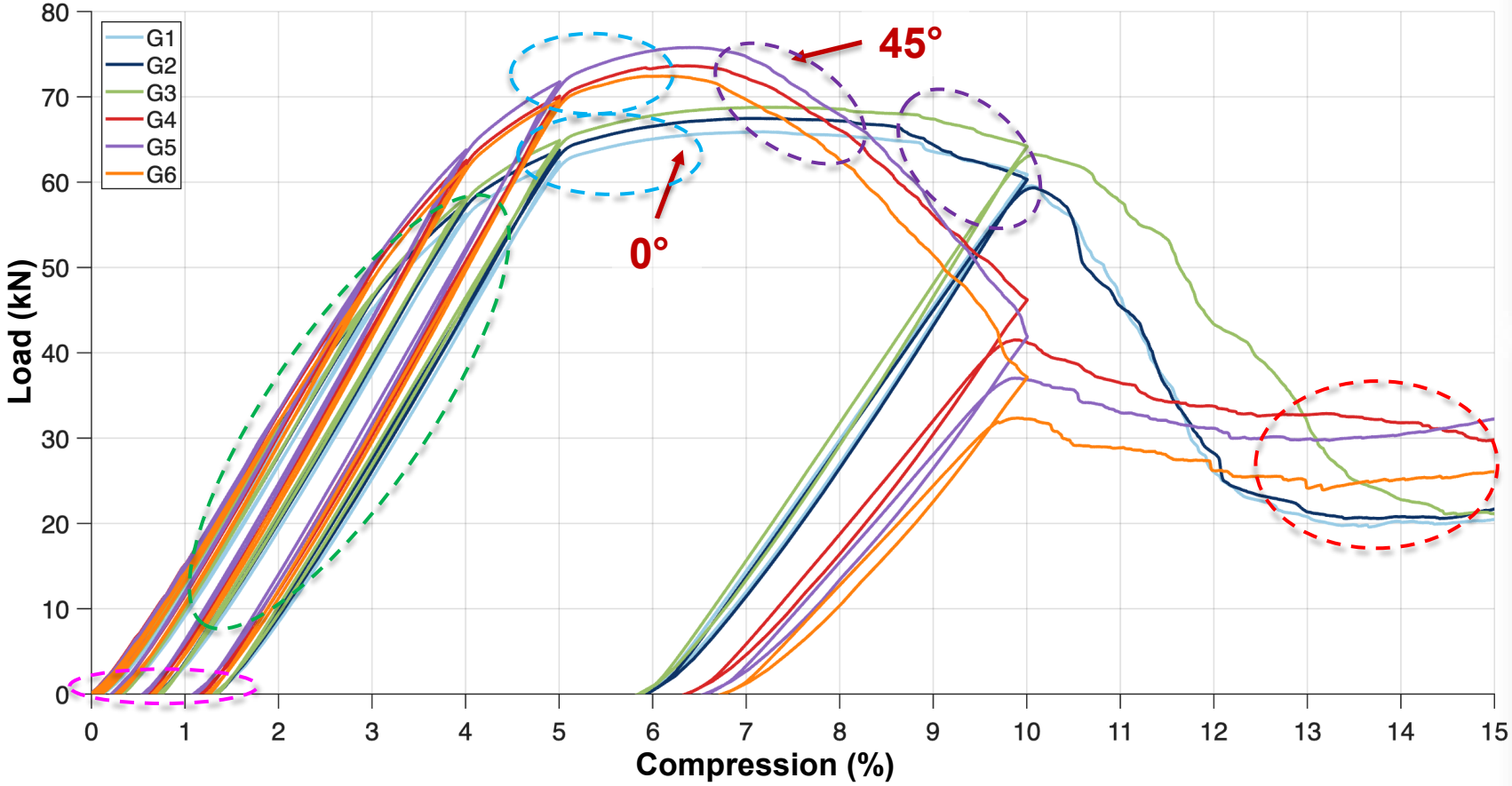


Fig. 21: Force–compression diagram of Gyroid cellular structures, showing loading/unloading response of samples G1–G6)

HEXAGONAL

Hexagonal: lower peak load and abrupt collapse behaviour

- Fmax ≈ 44–53 kN
- Peak reached at about 4–5.5% compression
- 45° orientation shows higher peak load
- Pronounced post-peak force drop
- Limited plateau behaviour and delayed force recovery

Hypothesized regions in the compression response of cellular structures (I initial settling), (II – elastic dominated), (III – cell walls begin to collapse), (IV - collapse of cell walls), (V - cell walls interact)

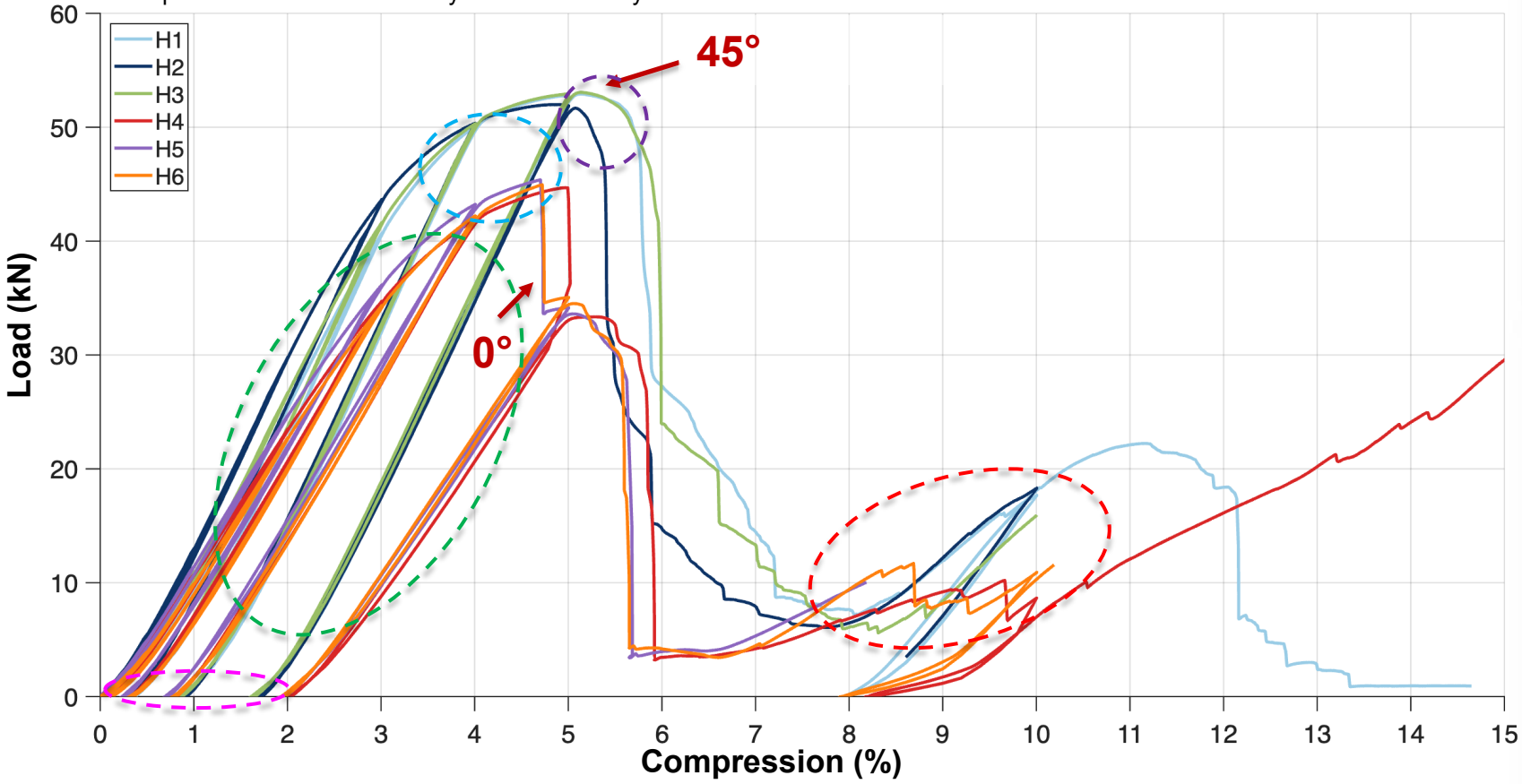


Fig. 22: Force–compression diagram of Hexagonal cellular structures, showing loading/unloading response of samples H1–H6)

FAILURE PATTERN IN COMPARISON: 0 °VS. 45 °

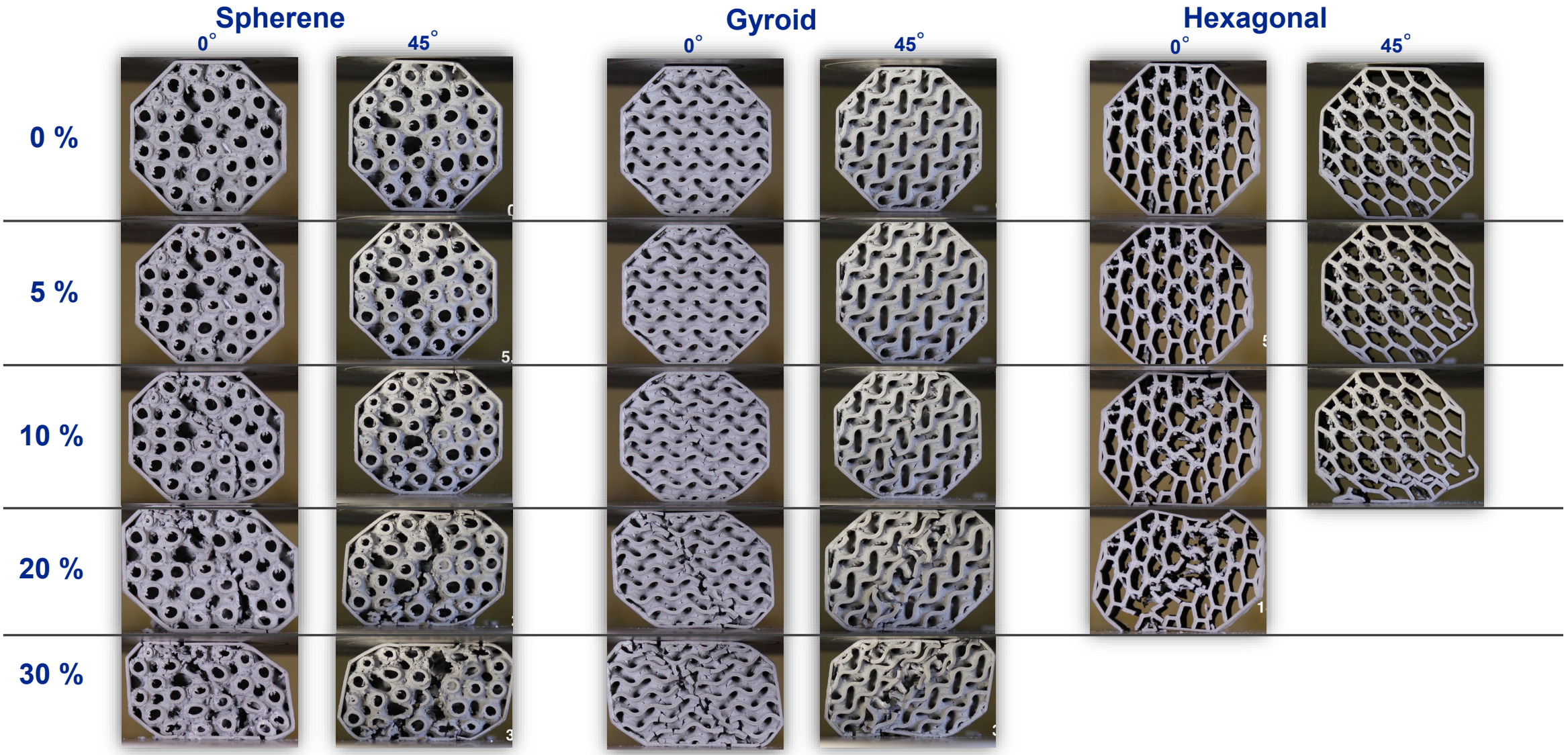


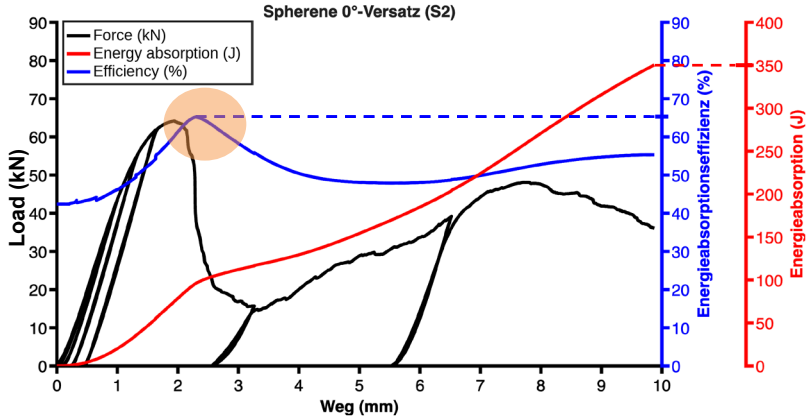
Fig. 23: Failure pattern of all infill types and samples

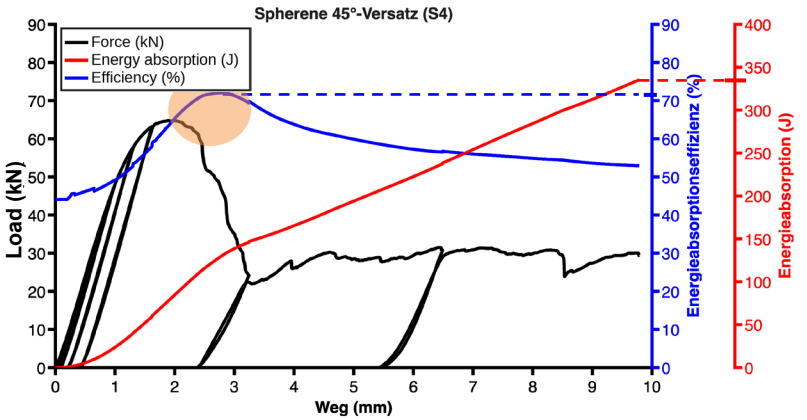
ENERGY ABSORPTION AND EFFICIENCY

Energy Absorption $E(\delta) = \int_0^{\delta} F(\delta)\,\mathrm{d}\delta$

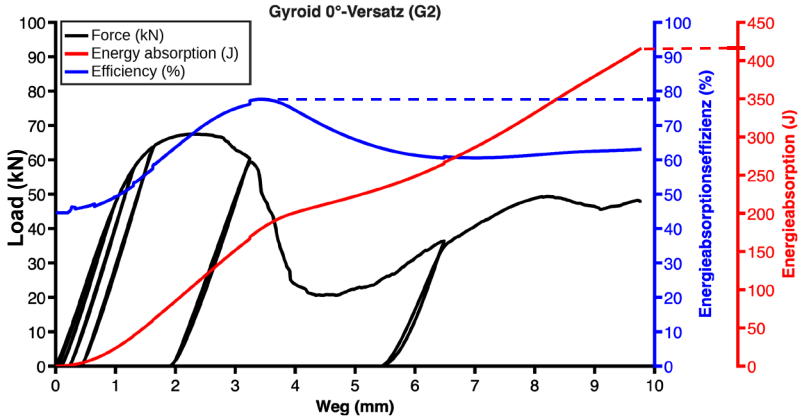
Energy Absorption Efficiency $\eta(\delta) = \frac{\int_0^{\delta} E(\delta)}{F_{\max}(\delta) \cdot \delta} \cdot 100\,\%$

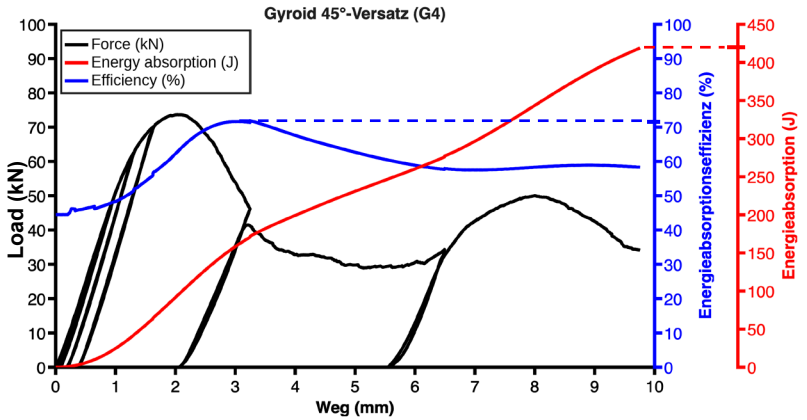
Spherene



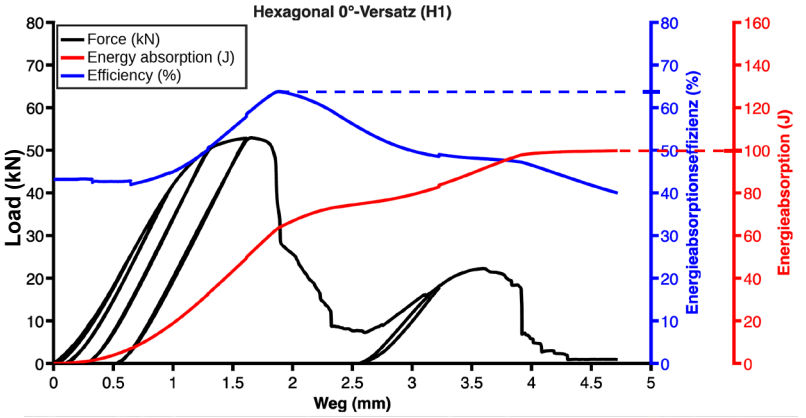


Gyroid





Hexagonal



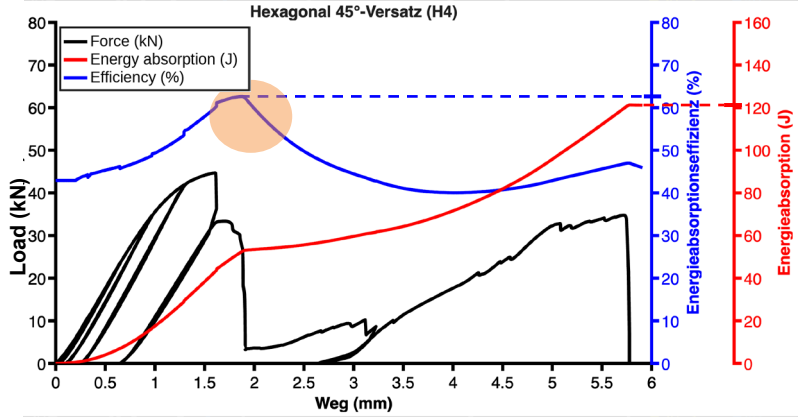


Fig. 24: Force-displacement and energy absorption and efficiency for each cellular structure and load direction

ENERGY ABSORPTION AND EFFICIENCY

$$SEA = \frac{\int_0^{\delta} F(\delta)\, d\delta}{m}$$

Deviations from 0° to 45°

Spherene:

- F_M= >5 %
- SEA = + 9.8%

Gyroid:

- F_M= + 10 %
- SEA = -11.6 %

Hexagonal:

- F_M= - 14.6 %
- SEA = -22.3 %

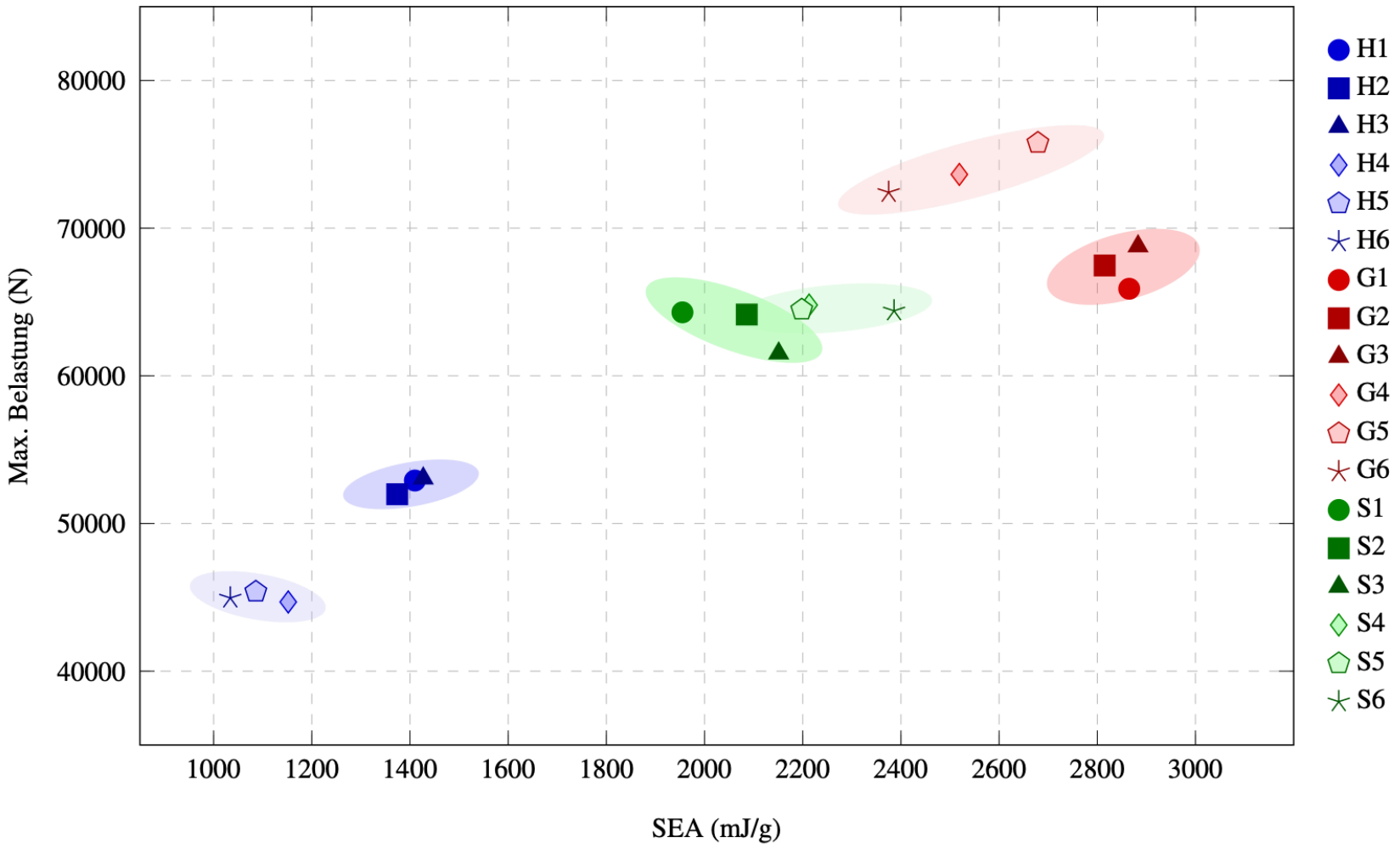


Fig. 25: Comparison of test results for maximum load and SEA (Specific Energy Absorption) between all samples

SUMMARY AND OUTLOOK

Overall
Great future for applying cellular structures in extrusion-based SBAM
Spherene ADMS and Gyroid perform higher maximum load and compressive strain than hexagonal
High potential for using not only in lightweight, also Shock-absorbing crash elements

✓ Slicer successfully developed

- Developed slicing strategy reduces number of retracts by ~80%
- Significantly improved print quality of sphere samples

✓ MFGF process chain fully documented

- Relative sinter density ~99 % - exceeds literature values
- Reproducible production of all three cellular structures

✓ Isotropy of the Spherene structure proven

- Maximum load difference 0° vs. 45°: only 1 % (< 5 % limit)
- SEA difference: 9.8% — failure pattern visually identical

✓ Structural comparison completed

- Spherene → isotropic, first choice for various load directions
- Gyroid → highest SEA (2.85 mJ/g) but anisotropic (±11.6%)

Outlook
FEM simulation
Improving spherene green part quality
Characterization for different cell design parameters
Analyzing cell collapse mechanism under compression load
Developing a homogenization approach
Using advantage of near-isotropy for structural and field optimization.

THANK YOU FOR YOUR ATTENTION!

FATIH GÖZÜKÜÇÜK
HAMBURG UNIVERSITY OF APPLIED SCIENCES

Gefördert durch:
Bundesministerium für Wirtschaft und Klimaschutz
aufgrund eines Beschlusses des Deutschen Bundestages

EMATec
International Conference on Emerging Applications of PM & AM Materials and Technologies

SIGNAL

HAW HAMBURG